Available online at www.sciencedirect.com
SCIENCE DIRECT®
Nuclear Instruments and Methods in Physics Research A 543 (2005) 114–117
NUCLEAR INSTRUMENTS & METHODS IN PHYSICS RESEARCH Section A
www.elsevier.com/locate/nima

Numerical modeling of the Novosibirsk terahertz FEL and comparison with experimental results

A.V. Kuzmin*, O.A. Shevchenko, N.A. Vinokurov

Budker Institute of Nuclear Physics, 11 Acad. Lavrentyev Prospect, 630090 Novosibirsk, Russia

Available online 2 March 2005

Abstract

Recently a new high-power terahertz FEL has been put in operation at the Siberian Center for Photochemical Research in Novosibirsk. In this paper, we use a simple 1-D model for numerical simulations of the FEL operation. The model is based on the excitation of multiple longitudinal radiation modes of the optical resonator by the charged discs. We restrict our consideration to the transverse fundamental modes only. The results of numerical simulations are in good agreement with analytical estimates and experimental data.

PACS: 41.60.C

Keyword: Free electron laser

1. Introduction

The Novosibirsk high-power FEL started operation recently [1]. It operates in CW mode at terahertz band using a simple two-mirror optical resonator. The computer code was created to provide simulations for all measured data. As the beam transverse sizes are significantly less than the radiation eigenmode size, it is enough to use a one-dimensional code.

2. Model description and basic equations

The electron beam in our model is presented as a set of thin rigid disks with Gaussian transverse distribution of charge, which is supposed to be the same for each disk. We neglect the influence of the radiation field on the transverse motion of a disk. We also neglect betatron oscillations and include their contribution to the longitudinal velocity as

*Corresponding author. Tel.: +7 3832 394859; fax: +7 3832 342163.
E-mail address: kuzmin@gorodok.net (A.V. Kuzmin).

0168-9002/$ - see front matter © 2005 Elsevier B.V. All rights reserved.
doi:10.1016/j.nima.2005.01.124

an additional energy spread. It is convenient to use the longitudinal spatial coordinate z as an independent variable. In this case, the system of equations for the longitudinal motion can be written as

$$\frac{d\tau_n}{d_z} = \frac{1}{V_z(\Delta_n)} - \frac{1}{V_z(0)}$$
$$\frac{d\Delta_n}{dz} = \frac{e}{\gamma_0 m_e c^2}\langle E_x\rangle x'(z) \quad (1)$$

where n is the disk number, $V_z(\Delta)$ is the longitudinal velocity, τ_n is the time delay with respect to the reference particle with energy γ_0, Δ_n is the relative energy deviation, and $\langle E_x\rangle$ is radiation electrical field, averaged over disk charge distribution. $x'(z)$ is the transverse trajectory angle in the x–z plane, in our approximation it depends only on the z coordinate, and in the case of planar undulator $x'(z) = -(K/\gamma_0)\sin(k_w z)$, where K is the undulator deflection parameter and k_w is the undulator wave number.

The radiation field inside the optical resonator may be represented as the linear combination of the resonator eigenmodes. Taking into account the small transverse size of the electron beam and the relatively high damping rate for high-order transverse modes, one can restrict the consideration to the fundamental transverse mode only. Then the on-axis radiation electric field may be represented as

$$E_x(0,0,z,t) = 2\mathrm{Re}\left[\sum_k a_k(z)e^{ik(z-ct)}\right] \quad (2)$$

For the numeric calculations, it is convenient to consider the discrete spectrum wave packet with the carrier wave number $k_0 : k_m = 2\pi m/cT_0 + k_0$, m is an integer, and T_0 is the envelope period. T_0 values have to be chosen much more than the packet duration (typically, of the order of the electron bunch length). Using this field expansion, one can derive the FEL equations for a single pass of the wave packet and particles (charged disks) through the undulator:

$$\frac{db_k}{d\theta} = \sum_n D e^{i[\theta\delta_k + \varphi_n(1+\delta_k)]}$$
$$\frac{d\Delta_n}{d\theta} = -\mathrm{Re}\sum_k b_k e^{-i[\theta\delta_k + \varphi_n(1+\delta_n)]}$$
$$\frac{d\varphi_n}{d\theta} = -2\Delta_n. \quad (3)$$

Here we introduced the following set of dimensionless variables and constants:

$$\varphi_n = k_0 c\tau_n,$$
$$\theta = k_w z,$$
$$\delta_k = \frac{k-k_0}{k_0},$$
$$b_k = -\frac{eK}{m_e c^2}\frac{(JJ)_0}{\gamma_0^2}\frac{i}{k_w}a_k,$$
$$D = \pi\frac{Q}{T_0 S_0 I_0 \gamma_0^3}\left[\frac{K(JJ)_0}{k_w}\right]^2,$$

where $(JJ)_0$ is the standard combination of Bessel functions, $I_0 = m_e c^3/e$ is the Alfven current, S_0 is an effective area of radiation (the power over the on-axis intensity), and $k_0 = 2\gamma_0^2 k_w/(1+K^2/2)$ is chosen.

One can easily check that system, Eq. (3) conserves the total energy

$$\frac{d}{dz}\left(\sum_k \frac{|b_k|^2}{2D} + \sum_n \Delta_n\right) = 0. \quad (4)$$

It also worth noting that this system can be derived from the Hamiltonian

$$H = -\sum_n \Delta_n^2 + \sum_n\sum_k \sqrt{\frac{2DI_k}{1+\delta_k}} \times \sin[\theta\delta_k + \varphi_n(1+\delta_k) - \psi_k] \quad (5)$$

where $I_k = |b_k|^2/2D(1+\delta_k), \psi_k = \arg(b_k); \psi_k, \varphi_n$ and I_k, Δ_n are canonical coordinates and momenta, respectively. Then the existence of the integral Eq. (4) follows from the invariance of Eq. (5) with respect to the transformation, $\varphi_n \to \varphi_n + \delta s$, $\psi_k \to \psi_k + (1+\delta_k)\delta s$.

3. Numeric approximation and computer code description

To obtain the numeric solution of Eq. (3) we used the following difference scheme:

$$b_k^{j+1} = b_k^j + hD\sum_n e^{i[\theta\delta_k + \varphi_n^j(1+\delta_k)]}$$

$$\Delta_n^{j+1} = \Delta_n^j - h\mathrm{Re}\sum_k \frac{b_k^{j+1} + b_k^j}{2} e^{-i[\theta\delta_k + \varphi_n^j(1+\delta_k)]}$$
$$\varphi_n^{j+1} = \varphi_n^j - 2h\Delta_n^{j+1} \quad (6)$$

where j is the step number and h is the step size. This scheme implements a canonical transformation of the phase space. It also conserves the following value:

$$\sum_k \frac{\left|b_k^j\right|^2}{2D} + \sum_n \Delta_n^j = const \quad (7)$$

which corresponds to the energy integral (4).

The computational algorithm, which directly followed from Eq. (6), was realized in a simple computer code. The code simulates reiterated passes of the radiation wave packet and the electron beam through the undulator. At the beginning of each pass, a new particle initial distribution is formed, and all amplitudes of the radiation field modes b_k are reduced with accordance to the losses of the optical resonator. The center of a new bunch is delayed by the optical resonator length L detuning $\delta T = 1/f_0 - 2L/c$ (f_0 is the bunch repetition rate). We used Gaussian distribution for energy Δ_n and uniform, parabolic or Gaussian distributions for coordinate φ_n. The typical number of radiation modes is 800 and the number of particles is 1000.

Accuracy of the code was checked for the small-signal low-gain calculations. The obtained dependences for the gain showed a very good agreement with the theoretical expressions. The results of simulation with the real FEL parameters are presented below.

4. Simulation results

Simulations were carried out with the Novosibirsk FEL parameters [1]. The dependence of the average radiation power inside the optical resonator on the pass number for different detunings is presented in Fig. 1. One can see that the radiation power reaches saturation after a few hundreds of electron bunches pass through the undulator. For some detunings there was no constant saturation level and the power was non-stationary.

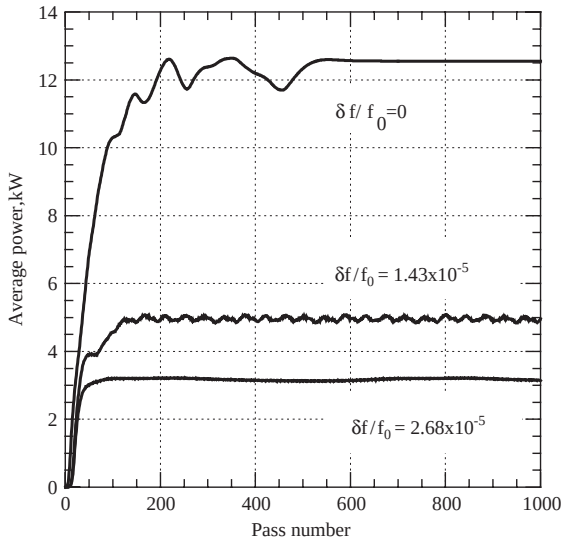

Fig. 1. Dependence of average radiation power inside the optical resonator on pass number for different detunings $\delta f/f0 = -c\delta T/(2L)$.

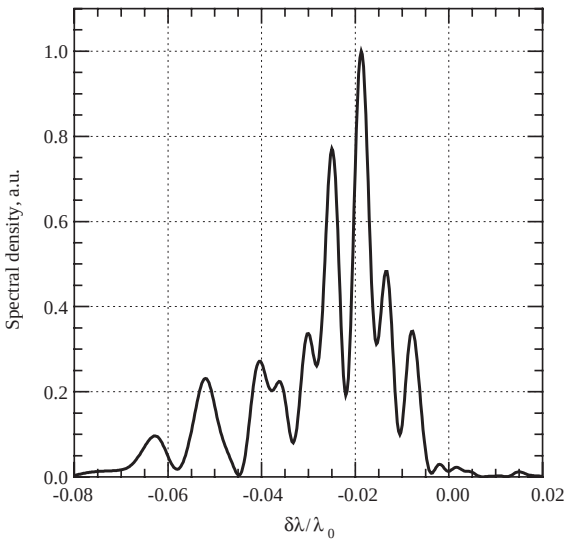

Fig. 2. Spectral density distribution for zero detuning.

The maximum level of average power inside the optical resonator at zero detuning is about 12 kW, which is in good agreement with the value obtained in the experiment.

Spectral density of radiation in the case of zero detuning is shown in Fig. 2. The presence of several bands in the spectrum apparently indicates the development of side-band instability.

The corresponding power distribution in the time domain is presented in Fig. 3. It can be seen that the radiation wave packet in this case consists of three short pulses. The distance between adjacent pulses is slightly shorter then total slippage at the undulator length. The mechanism

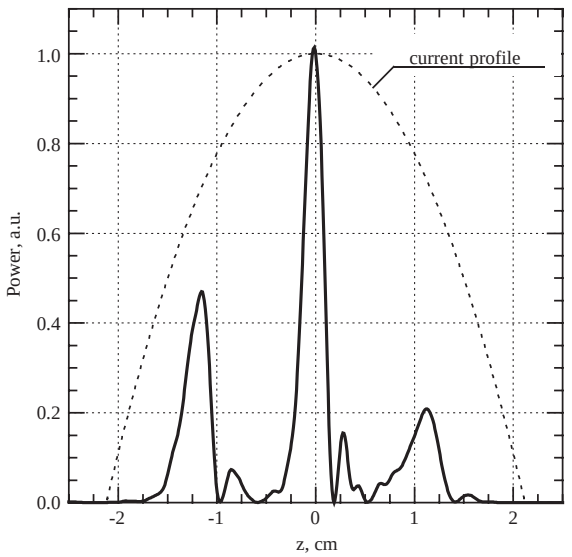

Fig. 3. Power distribution over the wave packet length for zero detuning. The dotted line corresponds to the beam current profile.

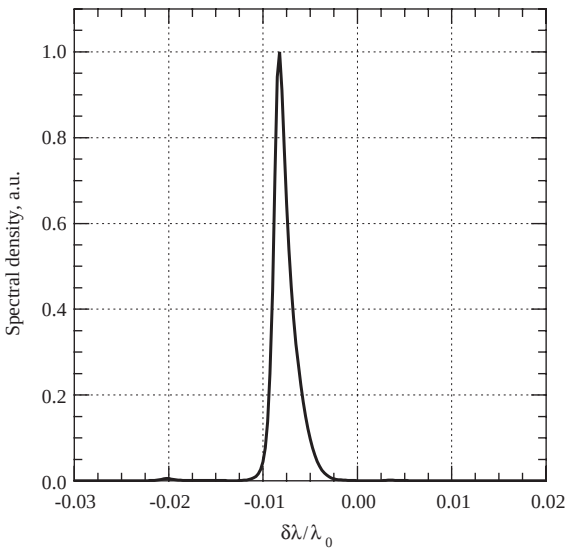

Fig. 4. Spectral density distribution for the detuning $\delta f/f_0 = 2.65 \times 10^{-5}$.

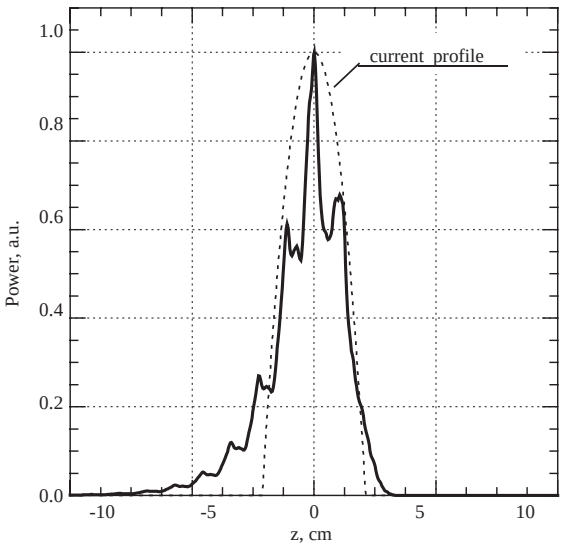

Fig. 5. Power distribution for the detuning $\delta f/f_0 = 2.65 \times 10^{-5}$.

of such short pulse generation was described analytically in Ref. [2].

For large enough nonzero detuning, the spectrum of radiation is narrow as is shown in Fig. 4. A similar spectrum with FWHM ~0.3% has also been observed in the experiment for some regimes.

Power distribution in the time domain for nonzero detuning is presented in Fig. 5. The wave packet length in this case is much longer than in the previous one.

5. Conclusion

The results of calculations demonstrate a good agreement with the measured ones. The lack of information about the particle distribution in the real electron beam is, probably, the main limiting factor for the comparison of the experimental data and the simulation results. Calculations for more advanced FEL magnetic systems (multisection and tapered undulators, optical klystron, electron outcoupling, etc.) are planned.

References

[1] E.A. Antokhin, et al., Nucl. Instr. and Meth. A 528 (2004) 15.
[2] N. Piovella, P. Chaix, G. Shvets, D.A. Jaroszynski, Phys. Rev. E 52 (1995) 5470.